




# Evaluation of ATAD2 as a Potential Target in Hepatocellular Carcinoma

Umut Ekin<sup>1,2</sup> · Haluk Yuzugullu<sup>3,4</sup> · Cigdem Ozen<sup>1,3,8</sup> · Peyda Korhan<sup>1</sup> · Ezgi Bagirsakci<sup>1,2</sup> · Funda Yilmaz<sup>5</sup> · Ozge Gursoy Yuzugullu<sup>3,4</sup> · Hamdiye Uzuner<sup>1,2</sup> · Hani Alotaibi<sup>1,2</sup> · Petek Ballar Kirmizibayrak<sup>6</sup> · Nese Atabey<sup>1,7</sup> · Gökhan Karakulah<sup>1,2</sup> · Mehmet Ozturk<sup>1,3,4,7</sup> 

Accepted: 7 October 2021 / Published online: 5 November 2021  
© Springer Science+Business Media, LLC, part of Springer Nature 2021

## Abstract

**Purpose** Hepatocellular carcinoma (HCC) is one of the leading causes of cancer-related death worldwide with lack of effective systemic chemotherapy. In this study, we aimed to evaluate the value of ATPase family AAA domain-containing protein 2 (ATAD2) as a biomarker and potential therapeutic target for HCC.

**Methods** The expression of ATAD2 was tested in different HCC patient cohorts by immunohistochemistry and comparative transcriptional analysis. The co-expression of ATAD2 and proliferation markers was compared during liver regeneration and malignancy with different bioinformatics tools. The cellular effects of ATAD2 inactivation in liver malignancy was tested on cell cycle, apoptosis, and colony formation ability as well as tumor formation using RNA interference. The genes affected by ATAD2 inactivation in three different HCC cell lines were identified by global gene expression profiling and bioinformatics tools.

**Results** ATAD2 overexpression is closely correlated with HCC tumor stage. There was gradual increase from dysplasia, well-differentiated and poorly-differentiated HCC, respectively. We also observed transient upregulation of ATAD2 expression during rat liver regeneration in parallel to changes in Ki-67 expression. ATAD2 knockdown resulted in apoptosis and decreased cell survival in vitro and decreased tumor formation in some HCC cell lines. However, three other HCC cell lines tested were not affected. Similarly, gene expression response to ATAD2 inactivation in different HCC cell lines was highly heterogeneous.

**Conclusions** ATAD2 is a potential proliferation marker for liver regeneration and HCC. It may also serve as a therapeutic target despite heterogeneous response of malignant cells.

**Keywords** Liver cancer · ATAD2 · Proliferation · Apoptosis · Gene expression profiles · Gene knock down

✉ Mehmet Ozturk  
mehmet.ozturk@ibg.edu.tr

- <sup>1</sup> Izmir Biomedicine and Genome Center, Izmir, Turkey
- <sup>2</sup> Izmir International Biomedicine and Genome Institute, Dokuz Eylul University, Izmir, Turkey
- <sup>3</sup> Department of Molecular Biology and Genetics, Bilkent University, Ankara, Turkey
- <sup>4</sup> Institut Albert Bonniot, Grenoble, France
- <sup>5</sup> Department of Pathology, Faculty of Medicine, Ege University, Izmir, Turkey
- <sup>6</sup> Department of Biochemistry, Faculty of Pharmacy, Ege University, Izmir, Turkey
- <sup>7</sup> Faculty of Medicine, Izmir Tinaztepe University, Izmir, Turkey
- <sup>8</sup> Present Address: Center for Molecular and Cellular Bioengineering, Technische Universität Dresden, Bioinformatics group, Dresden, Germany

## Introduction

The AAA + ATPase and bromodomain factor ATAD2/ANCCA (ATAD2) is composed of two AAA + domains and a bromodomain that recognizes acetylated histones [1]. As a nucleosomal protein present on active genes, its functions are closely associated with chromatin remodeling, DNA replication, and DNA repair. ATAD2 has been referred to as a “generalist facilitator of chromatin dynamics” based on demonstrations where histone acetylation guides ATAD2 to chromatin, resulting in an overall increase of chromatin accessibility and histone dynamics [2]. ATAD2 bromodomain was shown to recognize di-acetylated histones, and it associates with H4K5acK12ac modifications found on newly synthesized histones following DNA replication, suggesting a critical role for ATAD2 following DNA replication [3].

Based on structural studies with its yeast homolog, ATAD2 was proposed to form a hexameric complex and to facilitate H3-H4 loading by binding to histone tails [4]. Recently, Shahnejat-Bushehri and Ehrenhofer-Murray [5] reported that the yeast homolog of ATAD2 is a deposition factor for CENP-A homolog with help from HJURP homolog, thus acting as a co-chaperon for centrosome assembly.

ATAD2 has been described initially as a co-activator of the estrogen receptor overexpressed in breast cancer [6], and several other cancers [7], as well as a cancer/testis antigen [8]. Shortly after, we reported ATAD2 as a component of 15-hepatocellular immortality signature gene panel that discriminates hepatocellular carcinoma (HCC) from cirrhosis with high accuracy [9]. ATAD2 has now been implicated in a large set of cancer and been considered a therapeutic target [10].

Here, we studied the expression and functional implications of ATAD2 in liver malignancy in order to evaluate its potential as a potential target for HCC treatment. A series of investigations using gene and protein expression in normal and malignant tissues and cells, gene inactivation techniques, as well as in vitro and in vivo cell survival and tumorigenicity assays allowed us to draw critical conclusions about the value of ATAD2 as a therapeutic target for HCC with some implications that could be expanded to other cancer types overexpressing this particular epigenetic regulator.

## Material and Methods

### Cell Lines and Hepatocytes

Cell lines used in the study were obtained and cultivated as previously described [11]. Cell lines were maintained in RPMI medium supplemented with 10% Fetal Bovine Serum, 100 IU/ml penicillin, 100 µg/ml streptomycin and 1 × non-essential amino acid (ThermoFisher) under humidified 5% CO<sub>2</sub> and 37 °C conditions. Routine cell passages were performed when cell confluency reached to 70–80%. Freshly isolated human hepatocytes were obtained commercially (hNHEPSTM-Human Hepatocytes, Lonza Group, Basel, Switzerland), as reported previously [9].

### Generation of Polyclonal Anti-human ATAD2 Antibody

An anti-human ATAD2 antibody was generated in rabbits. The DNA fragment containing amino acids 2 to 251 at the N-terminus of the ATAD2 protein (Online Resource 1) was cloned into pET28 MHL plasmid vector. Briefly, the sequence to be cloned was amplified by polymerase chain reaction from a pCDNA3.1-HA-C plasmid carrying the

human ATAD2 cDNA. Primers used for this PCR: 5' TTG TATTTCCAGGGCGTGGTTCTCCGCAGCAGCTTG-3' and 5'-CAAGCTTTCGTCATCATTGGTCTTCACCCTC TTCAGATGAC-3'.

In-Fusion kit (Clontech) was used for cloning. pET28 MHL vector was cut with BseRI (R0581L, NEB) and purified with Nucleospin gel cleaning kit (Macherey–Nagel). Linear vector DNA and PCR-amplified ATAD2 DNA were mixed in the reaction medium at a ratio of 2:1. After ligation, the reaction solution was transformed into *E. coli* DH5α strain. The plasmid was transformed to *E. coli* T7 expression bacterial strain. Recombinant protein produced in bacteria was purified by Ni NTA agarose affinity chromatography using the non-soluble protein purification method. Rabbits were immunized with recombinant ATAD2 protein and rabbit sera were collected by CovalAb S.A.S. (Villeurbanne, France). Polyclonal antibody was purified using HiTrap Protein G HP ÄKTA FPLC system (GE Healthcare).

### Other Antibodies

The list of other antibodies used here was shown in Online Resource 2.

### Western Blotting

Harvested cell pellets were lysed in RIPA lysis buffer containing 150 mM NaCl, 1% Nonidet P-40, 0.5% Sodium deoxycholate, 0.1% SDS, 25 mM pH7.4 Tris, 1 × protease inhibitor cocktail (cOmplete, ROCHE), 1 mM Na<sub>3</sub>VO<sub>4</sub> and 1 mM NaF. Total protein amounts were measured and equalized according to BSA standard linear regression method. Equal amounts of denatured total protein samples were loaded to 10% SDS–polyacrylamide gels for electrophoresis. Transfers were performed to polyvinylidene difluoride membranes (immobilon-P, Millipore) and blocked with 5% non-fat milk. Membranes were probed with primary antibodies of targeted proteins and subsequently incubated with appropriate HRP-conjugated secondary antibodies. Detection of membranes was performed with enhanced chemiluminescence.

### siRNAs and Transfections

Different ATAD2-targeting siRNAs were used. The effects of ATAD2 knock-down on cell proliferation and apoptosis were tested using following siRNAs generated by Eurogentec (France). ATAD2 siRNA1: ACUAAACACUGCUGAAGCUG; ATAD2 siRNA2: GGUUGUAGCUCCUCCAAAU; ATAD2 siRNA3: GCUAAGGAUUUCGAGGUAG; ATAD2 siRNA4 UCUUCUGCUGUCAGUGAUC. Control siRNA (siCTRL); GGCCUUUCACUACUCCUAC. For transfections, cells were seeded in 6 well plates. After 24 h,

cells transfected with 100 pmol ATAD2 siRNAs and 4  $\mu$ l of oligofectamine transfection reagent (Invitrogen) for 6 h without serum and antibiotics. At the end of 6 h, media was changed and experiments continued as indicated for each test. The effects of ATAD2 knock-down on gene expression profiles were studied with transfection of ON-TARGETplus siRNAs (Dharmacon): S2: siRNA J-017603–06, Target Sequence: GUAAUCAGCCAAUGUAUUU, S3: siRNA J-017603–07, Target Sequence: CGUCGAAGUUGUAGG AUUA, S4: siRNA J-017603–08, Target Sequence: CUG AUGAGGUUCCUGAUUA, Control Luciferase Duplex, Target Sequence: CAUUCUAUCCUCUAGAGGAUG. Transfections were carried out according to supplier's instructions. Briefly, 500  $\mu$ l OptiMem (Thermofisher) and pool of 20 nM ATAD2 siRNAs 2, 3 and 4 were added to each well of 6-well plates and mixed gently. 5  $\mu$ l of Lipofectamine RNAiMax solution (Thermofisher) was added to each well and left to incubate for 20 min at room temperature by gently mixing again. Suspension of  $1 \times 10^5$  cells in 2.5 ml antibiotic-free medium was added to each well. At 48 h, cells were collected. ATAD2 knock-down was confirmed by real-time PCR of transfected cell RNAs using the following primers: ATAD2\_F-5'-TGAAAAGGCTTT GGCAATTC-3', ATAD2\_R-5'-TGCGATGCCGATAAA TACA-3', GAPDH\_F-5'-GGCTGAGAACGGGAAGCT TGTCAT-3', and GAPDH\_R-5'-CAGCCTTCTCCATGG TGGTGAAGA-3' were used for control experiments. Total Hep3B, SNU449, and PLC/PRF/5 RNAs used in microarray analysis were isolated with NucleoSpin RNA II Kit (MN Macherey–Nagel, Duren, Germany) and cDNA synthesis was performed using RevertAid First Strand cDNA synthesis kit (MBI Fermentas, Germany). Quantitative expression analyses were carried up with DyNAmo HS SYBR Green qPCR Kit F410 (Finnzymes). The reaction mix per well contained 10  $\mu$ l Sybergreen, 0.8  $\mu$ l of 10 pmol forward and reverse primers, 7.4  $\mu$ l ddH<sub>2</sub>O and 1  $\mu$ l cDNA. After adding mineral oil onto each well as 1:1, reaction carried out in Mx3005p PCR machine (Stratagene). The house-keeping gene, glyceraldehyde-3-phosphate dehydrogenase (GAPDH), was used as the internal control.

### Cell Proliferation, Colony Formation, and Apoptosis Studies

HCC cells were seeded in 6 well plates. After 24 h, cells transfected with 100 pmol ATAD2 siRNAs and 4  $\mu$ l of oligofectamine (Invitrogen) transfection reagent for 6 h without serum and antibiotics. At the end of 6 h, media with 3  $\times$  serum added on. Cells were monitored for 96 h and stained with Coomassie blue at the end of the experiment. For colony formation studies, Hep3B and HepG2 cells were seeded at 72 h following transfection, and grown for 10 days for colony formation. Colonies were stained with crystal

violet and quantified. Similarly, Hep3B, HepG2, Huh7 and Hep40 cells were treated with siRNAs of ATAD2 and cultured for 3 days. Cells suspended and pelleted by centrifugation. Cells washed with PBS and fixed with ice cold ethanol. Ethanol discarded and cells washed with PBS. Cells treated with RNase A (Fermentas) and stained with propidium iodide (Sigma). In Annexin V staining, Hep3B and HepG2 cell pellets resuspended with Annexin V binding buffer and stained with Annexin V-Cy3 dyes (Sigma Aldrich). After 5 min incubation at dark, FACS scan (Beckton Dickonson) with FL2 channel was used for analysis.

### Clinical Tissue Specimens and Immunohistochemistry

Normal liver and HCC tumor samples were collected and analyzed at Ege University Department of Pathology under the ethical approval. In total, 7 normal liver, 9 low grade dysplastic nodules (LGDN), 18 high grade dysplastic nodules (HGDN), and 27 HCC samples were identified. The diagnosis of dysplastic nodules and HCC, as well as HCC grading, was made according to previously defined criteria [12]. Immunohistochemical analyses were performed on 5  $\mu$ m-thick sections taken on positively charged slides. Sections were deparaffinized in xylene and then rehydrated. Immunohistochemical staining for anti-ATAD2 antibody (HPA029424, Sigma, 1:150 dilution) was performed using an automated immunohistochemical stainer according to the manufacturer's guidelines (streptavidin-peroxidase protocol; BenchMark, Ventana, PA, USA). The immunoreactivity was revealed by 3, 3-diaminobenzidine tetrahydrochloride (DAB) staining and the sections were counterstained with hematoxylin. The intensity and extent of staining were evaluated semi-quantitatively.

### Immunofluorescence

First, a pool of ATAD2 siRNAs or control siRNAs were mixed with Lipofectamine RNAiMax solution (Thermofisher) in serum-free RPMI and left for 10 min at room temperature. Transfection media was mixed with cell suspension (5000 cells/well in RPMI) in 24-well plates containing coverslips. Cells were then incubated for 48 h. To stop the experiment, cell wells were washed with PBS and fixed with ice-cold Acetone-Methanol mixture (1:1) for 10 min at  $-20$  °C. Fixative was discarded and coverslips washed with PBS. Cells blocked for 30 min with PBS-T (PBS and 0.1% Triton-X) complemented with 1% BSA. Cells were co-incubated with primary antibodies to Ki-67 and ATAD2 diluted in PBS-T containing 0.5% BSA for 2 h at room temperature with gentle agitation. Cells were then washed and co-probed with fluorescence tagged anti-mouse and anti-rabbit secondary antibodies diluted in PBS-T containing

0.5% BSA for 90 min. Cells were washed, incubated with DAPI, rinsed with dH<sub>2</sub>O and mounted on slides with mounting media.

### Study of ATAD2 Response to Cell Stress

Hep3B and HepG2 cells were seeded on 60 mm dishes and incubated for 48 h. When they reached a confluence of 60–70% at 48 h, media were changed with fresh media containing tunicamycin (5 µg/ml and 10 µg/ml) per vehicle. Tunicamycin stock solution was dissolved in DMSO. After 12 h and 24 h treatments, cells were collected, and used for total protein extraction using RIPA buffer.

### Comparative Analysis of ATAD2 and Ki-67 Expression

We analyzed the relationship between ATAD2 and Ki-67 expression in rat liver with publicly available microarray gene expression data (GEO Accession: GSE63742) generated from rat liver during regeneration following partial hepatectomy. To analyze the expression data, we used GEO2R (<https://www.ncbi.nlm.nih.gov/geo/geo2r/>) web based interactive tool. The highest expression values with the “Probe Set 1374775\_at” for Mki-67, the “Probe Set 1376599\_at” for Atad2 genes were used respectively. Means and Standard Deviations (SD) of expression data for each time points were used for reporting. The correlation between ATAD2 and Ki67 expression in hepatocellular carcinoma was analyzed using TCGA LIHC tumor dataset available at UCSC Xena Browser [13]. Data of recurrent tumor samples were excluded from downstream analysis steps. The expression of ATAD2 and MKi67 was analyzed in 50 normal solid tissue and 371 primary solid tumors of liver. The correlation between ATAD2 and MKi67 is determined with Pearson’s correlation method. The following R packages were used in analysis of expression data and generating graphs are dplyr (v1.0.4), ggplot2 (v3.3.3) and ggpubr (v0.4.0).

### Generation of Doxycycline-Induced shATAD2 Expression Clones

The lentiviral constructs, pTRIPz shRNAmir lentiviral vector targeting ATAD2 or shControl were used (Open Biosystems company, Huntsville, USA) in the generation of Hep3B stable clones. The sequences in the constructs used as: Targeting shRNA: pTRIPz-tet-shRNA-ATAD2, 5'-ATT ACAGTGACATAATCAG-3' and NonTargeting Control RNA: pTRIPz-tet-shRNA-nontargeting control, 5'-AATTCT CCGAACGTGTACACGT-3'. These doxycycline-inducible constructs also include Red Fluorescent Protein (RFP) cassette that led to track cells. The lentiviral constructs transfected with Arrest-in transfection reagents (Open-biosystems

Company, Huntsville, USA) to HEK293TA cells. Cells treated with reagent-construct complex in media for 6 h and media refreshed. After 48 h, virus-containing supernatants collected and filtered by 0.45 µm PVDF filters for use. Hep3B cells seeded on 24 well plates before the day of transduction. At the day of transduction, media refreshed with virus containing media with Hexadimethrine Bromide Sigma (St. Louis, MO, USA). After 6 h incubation, virus containing media refreshed with fresh media. After 24 h, cells cultured with media containing 1 µg/ml puromycin (Sigma, St. Louis, MO, USA) to generate stable clones.

### Tumorigenicity Assays

In the generation of xenograft models, shControl and shATAD2 clones of  $10 \times 10^6$  Hep3B cells resuspended in phosphate-buffered saline and injected to both sides of 6 Female athymic NMRI nude mice (Janvier, Le Genest-Isle, France). Doxycycline (Sigma, St. Louis, MO, USA) dissolved in drinking water of 3 mice to induce expression of shControl and shATAD2. Size of the tumors measured every 3 or 4 days and graphed using Graphpad Prism V8. RFP expressing tumors were visualized by IVIS Kinetic device (Caliper Life Sciences) in vivo imaging system before mice sacrificed. Tumors of mice extracted for western blot analysis.

### Gene Expression Profiling by Microarrays

Total RNAs of siRNA-transfected cells were first tested with the Agilent Bioanalyzer 2100 for quality control. Only samples with RNA integrity number values (RIN) greater than 9 were used in microarray experiments. Affymetrix microarray system was used as described in our previous study [9]. Briefly, Affymetrix platform with GeneChip Human Genome U133 Plus 2.0 arrays were used for microarray analysis according to manufacturer instructions. In order to collect and store data, Operating Software (Affymetrix) was used. Bioinformatic analysis of microarray data was performed with R statistical computing environment (v3.6.1). Raw probe intensities in CEL files were subjected to robust multichip average normalization (RMA) using `expresso` function of Bioconductor `affy` package (v1.68.0) [14]. Differential expression analysis was performed with `Limma` package (v3.46.0) [15] to measure significant changes in gene expressions across pairwise comparisons. In this step, `lmFit` function was utilized to fit a linear model, and estimated coefficients and standard errors were then computed with `contrasts.fit` function. Empirical Bayes statistics were obtained using `eBayes` function. We considered differentially expressed genes using a fold change cutoff  $\geq 2$ . The Gene Ontology (GO) enrichment analysis of differentially expressed genes was performed with `clusterProfiler` package



(v3.14.3) [16] and the GO terms with  $FDR \leq 0.05$  were considered significant.

## Statistical Analysis

Graphs were generated with Prism 8 (Graphpad Software, La Jolla California, USA) and Microsoft Office Excel (2016). Group comparisons were analyzed with t tests. The differences between groups were considered statistically significant as  $*p \leq 0.05$ ,  $**p \leq 0.01$ , and  $***p \leq 0.001$ .

## Results

### ATAD2 is Over-expressed in HCC Tumors in a Tumor Grade Dependent Manner

To assess the clinical relevance of ATAD2 in HCC, we surveyed its expression by immunohistochemistry in 7 normal liver tissues, 9 low-grade dysplastic nodules (LGDN), 18 high-grade dysplastic nodules (HGDN) and 27 HCC cases. ATAD2 was expressed in 3 (16.7%) HGDN, and 14 (51.9%) HCC cases. There was no detectable ATAD2 expression in normal liver and LGDN. Thereafter, we observed a gradual increase in the percent of ATAD2-positive cells according to HCC grade. ATAD2 expressions in well-, moderate-, and poorly differentiated HCC were 25.0%, 66.7%, and 83.3%, respectively (Fig. 1a and Table 1).

### Strong Correlation Between ATAD2 and Ki-67 Expression in HCC as well as in Regenerating Liver

Next, we compared ATAD2 expression at RNA levels with that of Ki-67 transcripts encoded by *MKI-67* gene using The Cancer Genome Atlas (TCGA) data available at UCSC Xena Browser [13]. As shown in Fig. 1b, both transcripts were upregulated significantly ( $p < 0.001$ ) in HCC samples ( $n = 371$ ) as compared to non-tumor liver samples ( $n = 50$ ). Based on expression similarities between ATAD2 and *MKI-67*, we also performed Pearson correlation analysis for their co-expression in normal liver and HCC samples (Fig. 1c). We observed a significant correlation between ATAD2 and *MKI-67* expression ( $R = 0.61$ ,  $p < 2.2e-16$ ). The data we obtained with clinical tissue samples strongly suggested that ATAD2 expression in liver is related to cell proliferation, similarly to *MKI-67* expression. To further explore this correlation, we compared ATAD2 expression with the expression of two cell proliferation markers namely *CCND1* (encoding for Cyclin D1 protein) and *MKI-67* during experimental liver regeneration induced in rats by partial hepatectomy using a microarray expression dataset (GEO Accession: GSE63742) available at GEO database [17]. As shown in Fig. 1d, all three transcripts were low at the beginning of

the regeneration process and all of them displayed a peak of expression between 24 and 36 h. *CCND1* showed another increase at 72 h. Thereafter there was slow but progressive decrease in the levels of ATAD2, *MKI-67*, and *CCND1* transcripts, which came down to initial levels at 168 h or 7 days. Thus, there was a perfect correlation in the dynamic expression patterns of ATAD2 and cell proliferation markers *CCND1* and *MKI-67* in regenerating liver.

### Differential Expression of ATAD2 in Hepatocytes and HCC Cell Lines

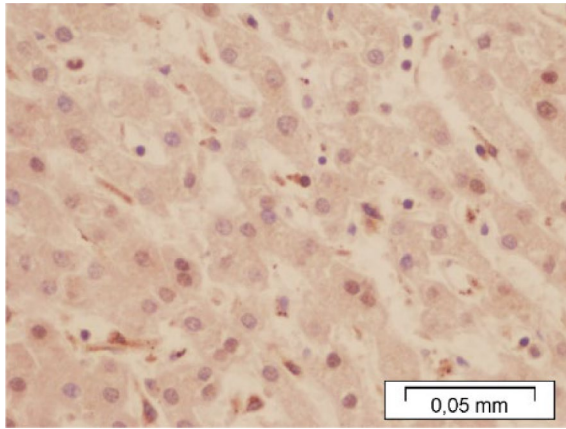
We reported previously that ATAD2 protein was not detectable by Western blotting in freshly isolated human hepatocytes, in contrast to consistent expression in HCC cell lines [9]. Here we confirmed and complemented these data by immunocytochemistry (Fig. 2a) and immunofluorescence studies (Fig. 2b). Non-proliferating hepatocytes lacked ATAD2 expression whereas HCC cell lines in culture displayed almost 100% positive nuclear staining. As demonstrated with SNU449 cell line, this nuclear positivity was specific to ATAD2 because of its attenuation under ATAD2 siRNA treatment (Fig. 2b left panels).

ATAD2 staining showed a good correlation with nuclear Ki-67 staining, a proliferation marker largely used for tumor pathology (Fig. 2b—middle panel). Taken together, in vivo and in vitro studies reported here clearly demonstrated that ATAD2 expression in liver is not specifically related to liver malignancy and correlated directly with the proliferation state of this tissue.

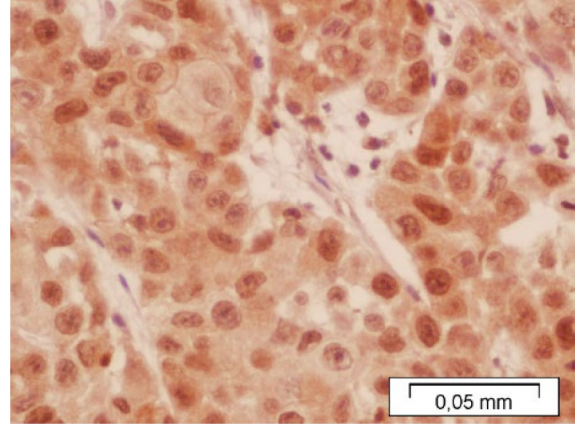
### ATAD2 Expression Is Downregulated Following Tunicamycin-Induced Unfolded Protein Response

One of the cellular consequences of Endoplasmic Reticulum (ER) stress is Unfolded Protein Response (UPR) which leads to the exit from the cell cycle through downregulation of Cyclin D1 levels [18]. Based on this finding, we aimed to test whether ATAD2 levels are also downregulated during UPR induced by tunicamycin, an inhibitor of protein glycosylation, triggering ER stress [19]. Hep3B and HepG2 cells were treated with 5  $\mu\text{g/ml}$  or 10  $\mu\text{g/ml}$  tunicamycin for 12 h or 24 h and cell lysates were tested for expression of CHOP, an indicator of Endoplasmic Reticulum (ER) stress induced by tunicamycin and PARP cleavage, an indicator of apoptosis together with ATAD2 abundance (Fig. 3). Both Hep3B and HepG2 cells responded to tunicamycin with early (12 h) induction of CHOP as expected. The accumulation of cleaved PARP was detected at 12 h in Hep3B cells with a strong increase at 24 h. HepG2 cell response was less pronounced with detectable PARP cleavage at 24 h only. ATAD2 levels showed a late decrease (24 h) in Hep3B, but early response (12 h) in HepG2 cells. These results suggest

**a**

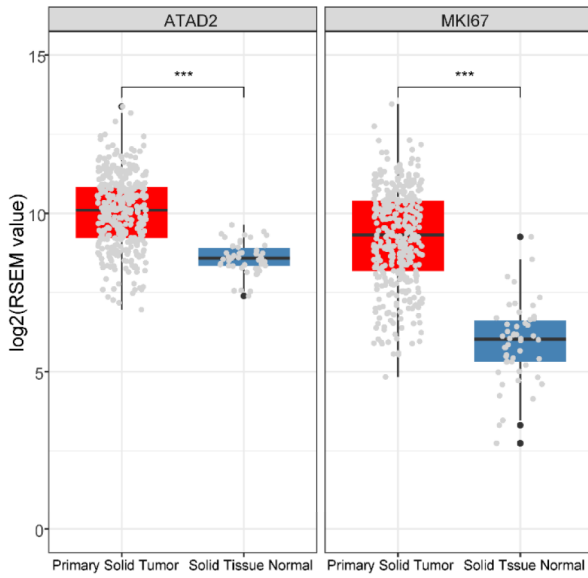


Normal liver

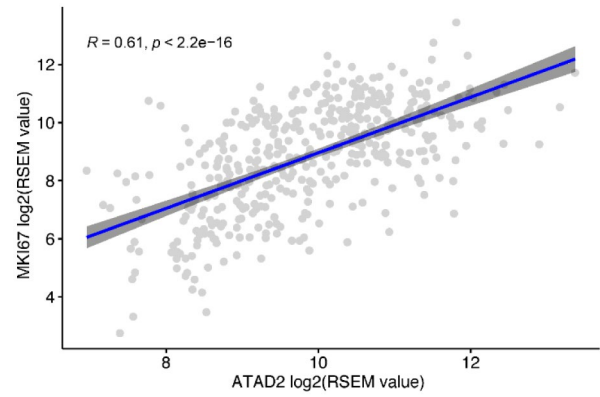


HCC

**b**



**c**



**d**

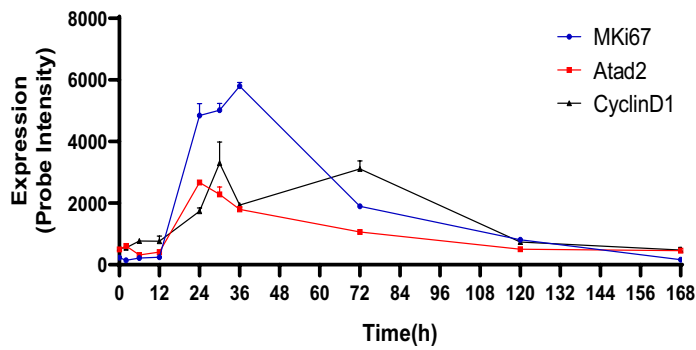


**Fig. 1** ATAD2 expression is induced in human HCC and during liver regeneration in correlation with Ki-67. **a** Representative immunohistochemical images of ATAD2 expression in human normal liver (left) and HCC (Right). **b** Both ATAD2 and Ki-67 transcripts are induced significantly in normal liver and HCC samples in TCGA collection. **c** Highly significant correlation between ATAD2 and Ki-67 expression in HCC. MKI67: Human gene encoding Ki-67. **d** ATAD2 expression during rat liver regeneration display similar profile with the profile of proliferation biomarkers Cyclin D1 and Ki-67, as shown by transcript analysis. MKi67: Rat gene encoding Ki-67

that when cell cycle arrest/apoptosis is triggered, ATAD2 levels are going down.

### ATAD2 siRNA Treatment Inhibits HCC Cell Survival in Some but not All HCC Cell Lines

Based on close association between ATAD2 expression and hepatocellular proliferation, we sought to know whether ATAD2 is essential to HCC cell survival. We transfected a set of HCC cell lines with *ATAD2* siRNAs and followed their growth and survival. Out of five cell lines tested, Hep3B and HepG2 showed strong growth inhibition. SNU449 displayed only weak growth inhibition, whereas Huh7 and PLC/PRF/5 showed no noticeable change (Online Resource 3).

To investigate the functional consequences of *ATAD2* depletion, we transfected Hep3B and HepG2 cells with two different siRNAs. ATAD2 immunoblotting confirmed successful knock-down of *ATAD2* (Fig. 4a). Western blot analysis of cleaved caspase-3 protein (Fig. 4a) and detection of up to 30% Annexin V positive cells by flow cytometry suggested ATAD2 depletion induces apoptosis (Fig. 4b). These cell lines also reacted to *ATAD2* suppression with drastic changes in cell cycle phase distribution with accumulation of subG1 cells, supporting our previous observation (Fig. 4c). As a result, survival of Hep3B and HepG2 decreased significantly as assessed by colony formation assays (Fig. 4d).

Next, we expanded our investigations on in vivo effects of ATAD2 silencing using Hep3B cells, which responded strongly to *ATAD2* depletion. Due to the deleterious effects of *ATAD2* silencing, we chose a Doxycycline-inducible shRNA expression technique. Hep3B cells were first marked with stable expression of red fluorescent protein (RFP); then, we generated ATAD2 shRNA and control shRNA stable cell lines. shCTRL- and shATAD2-expressing Hep3B cells injected subcutaneously into the right and left sides of mice, allowed the tumors to grow for 2 weeks and shRNA expression triggered by including Doxycycline into drinking water (Fig. 5a). Tumor samples isolated at the end of the study validated successful ATAD2 knock-down (Fig. 5b). Doxycycline-treatment of mice led to significant tumor growth inhibition in shATAD2 tumors with respect to shCTRL ( $p = 0.0064$ , Fig. 5c). This effect was further

demonstrated by reduced RFP signals from ATAD2shRNA-expressing tumors using live imaging (Fig. 5a).

We selected Huh7 as a representative of HCC cell line whose survival did not show robust change upon ATAD2 siRNA treatment (Online Resource 3). As shown in Fig. 6, despite effective decrease of ATAD2 levels by ATAD2 siRNAs (Fig. 6a), there was no consistent change in cell cycle distribution. Of particular interest, subG1 signal, representing apoptotic cells, did not show any indication of increase (Fig. 6b, c).

### Gene Expression Response of HCC cells to ATAD2 Is Highly Heterogeneous

Phenotypic heterogeneity of different HCC cell lines in their response to ATAD2 depletion warranted further investigation. Therefore, we decided to compare global gene expression profiles of three different HCC cell lines in the presence as well as under suppression of ATAD2 expression. We chose Hep3B (high response), PLC/PRF/5 (medium/no response) and SNU449 (medium/no response) cell lines and used Affymetrix microarray technology. All cell lines were analyzed after 48 h of ATAD2 siRNA treatment as compared to control siRNAs. Effective downregulation of ATAD2 levels by siRNAs were demonstrated by real-time PCR (Fig. 7).

Expression levels of RNAs were compared between ATAD2 siRNA- and control siRNA-treated cells, and genes displaying more than twofold changes were identified. As expected, ATAD2 mRNA levels decreased 11, 11, and fourfold in Hep3B, PLC/PRF/5 and SNU449 respectively. ATAD2 knock-down resulted in the downregulation for 57 genes, while 54 displayed upregulation in Hep3B. The number of affected genes was much lower in PLC/PRF/5 cells (9 up and 7 downregulated respectively, while it was nil in SNU449 cells (Table 2). In order to find out what gene functions are affected by these changes, GSEA was utilized using gene ontology (GO) terms. As shown in Table 3, 11 GO terms all related to three diverse functions, namely lipoprotein particle remodeling, positive regulation of Wnt signaling pathway and Receptor-mediated endocytosis were identified for PLC/PRF/5 cells ( $p < 0.05$ ). Much higher number of gene functions were identified in Hep3B cells (33 GO terms with  $p < 0.02$ ). These functions were highly heterogeneous and grouped into 17 gene functions. Top affected functions were response to calcium ions, metal ions, ketone, glucocorticoid and cAMP, positive regulation of protein kinase B signaling, negative regulation of blood coagulation, negative regulation of ion transport, zymogen activation, and apoptosis pathway (Table 3). There was no commonality between the GO terms identified in Hep3B and PLC/PRF/5 cells.

**Table 1** Immunohistochemistry staining analysis of ATAD2 protein in normal liver, dysplastic nodules and HCC

| Differentiation | Total | Positive | % positive |
|-----------------|-------|----------|------------|
| Normal liver    | 7     | 0        | 0.0        |
| LGDN            | 9     | 0        | 0.0        |
| HGDN            | 18    | 3        | 16.7       |
| WD HCC          | 12    | 3        | 25.0       |
| MD HCC          | 9     | 6        | 66.7       |
| PD HCC          | 6     | 5        | 83.3       |

### Discussion

We identified ATAD2 several years ago as a member of senescence-related 15-gene signature set providing high confidence prediction of HCC patients with 97.5% accuracy [9]. In the same report, we also showed that freshly isolated human hepatocytes lack detectable ATAD2 protein in contrast to nine different HCC cell lines all expressing it. Here we evaluated the value of ATAD2 as a disease biomarker and potential therapeutic target for HCC. Our observations clearly indicate that this protein is a good disease progression marker, but a conditional therapeutic target.

**Fig. 2** ATAD2 is highly expressed in proliferating HCC cells, but not in non-proliferating hepatocytes. **a** Immunohistochemistry images show the absence of detectable ATAD2 protein in non-proliferating hepatocytes in contrast to Huh7 cells. **b** Immunofluorescence imaging of HCC cells indicating nuclear staining of ATAD2 mirroring Ki-67 staining

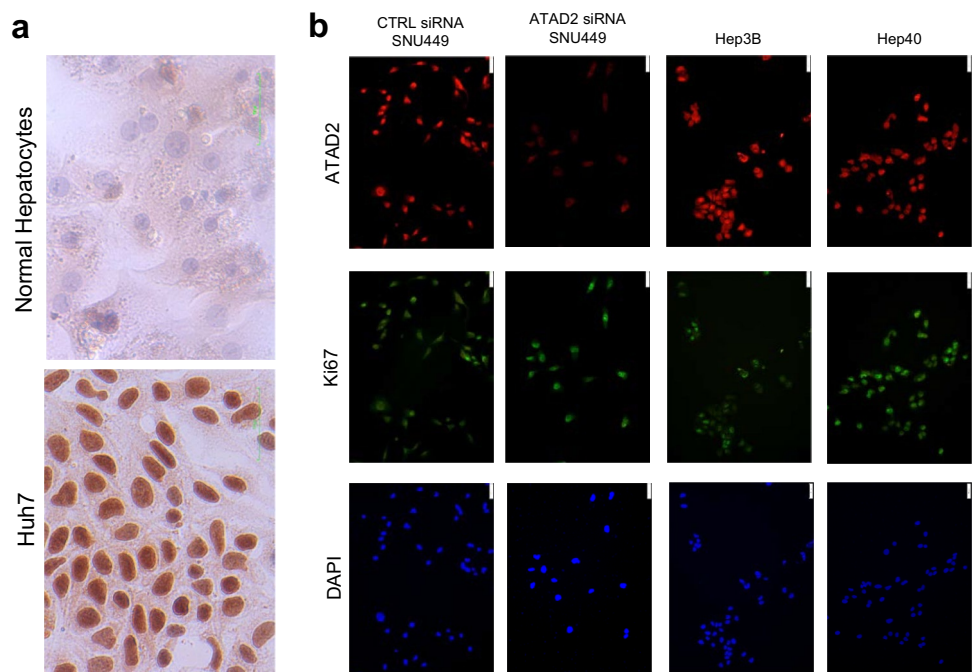
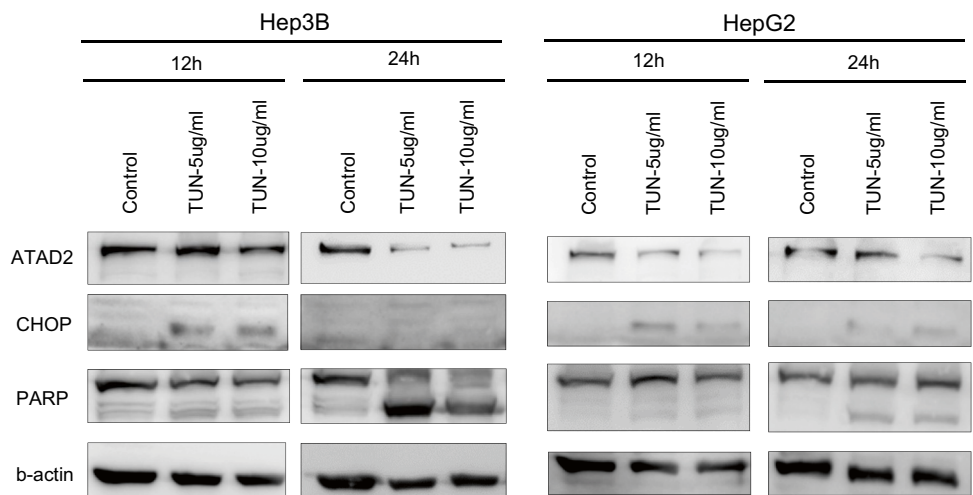


**Fig. 3** Western blot analysis of Hep3B and HepG2 cells under UPR induced by tunicamycin treatment. Note the decreased expression of ATAD2 in late phase (24 h) coinciding with strong apoptosis in Hep3B cells. In contrast HepG2 cells responded to tunicamycin with less apoptosis but early (12 h) inhibition of ATAD2 expression





The value as a tumor marker was evaluated using a set of tissues representing normal liver, dysplastic nodules and well-, moderate-, and poorly differentiated HCCs. We observed almost a perfect correlation between ATAD2-positive staining cell numbers and disease progression. Accordingly, ATAD2 was not detected in LGDNs but was positive in 17% of HGDNs. This positivity progressively increased up to 83% in poorly differentiated HCCs. Our observations correlate with data reported previously [20–22]. Here we provide novel data showing that ATAD2 expression in normal liver and HCC is closely correlated with Ki-67 expression, a well-known biomarker used to evaluate proliferation index in tumors [23]. This led us to consider ATAD2 as a proliferation biomarker. Next, we tested whether *ATAD2* expression in liver is specific to malignancy. Thus, we analyzed the status of its expression following induction of liver regeneration by partial hepatectomy in rats. This analysis was done in parallel to *MKI-67* and *CCND1* expression. *ATAD2*, *MKI-67*, and *CCND1* RNA levels were low in the initial phase of the liver regeneration and all three showed strong induction between 24 and 36 h, followed by a gradual decrease until the end of proliferation process. The absence of *ATAD2* expression in normal liver together with its increased expression in regenerating rat liver, as well as in malignant liver lesions as a function of tumor progression is reminiscent of Ki67 expression in these situations. Indeed, Ki67 labelling index (LI) is less than 5% in normal liver and inactive cirrhosis, but higher in chronic hepatitis (LI: 29–41) and very high (LI: 71) in HCC [23]. In confirmation of our observations, *MKI-67* expression during rat liver regeneration is induced and remained high for at least 4 days [24]. Ki-67 is a nuclear protein expressed in proliferating (G1, S, G2 and M phases) cells, but not in resting (G0 phase) cells including hepatocytes [25].

Our in vitro studies confirmed that ATAD2 is indeed a specific nuclear marker for proliferating cells like Ki-67. As shown in Fig. 2, normal hepatocytes did not express ATAD2, but all tested HCC cell lines displayed nearly 100% positive staining which paralleled Ki-67 staining. Indeed, ATAD2 immunostaining performs better than Ki-67 staining because of its homogenous nuclear staining pattern. The presence of nuclear ATAD2 in all proliferating cells despite its role in “co-chaperon” role in the organization of newly loaded histones during DNA synthesis [3] is not necessarily contradictory. Ki-67, a well-known marker for cells in proliferation (G1, S, G2, M phases) serves as a biological surfactant to disperse mitotic chromosomes during M phase [26].

Tunicamycin which causes extensive protein misfolding and activation of the unfolded protein response (UPR) is an ER-stress inducer [19, 27]. One of the cellular responses to UPR is to exit from the cell cycle by downregulation of Cyclin D1 levels [18]. Cyclin D1 degradation is also necessary for exit of hepatocytes from cell cycle and termination

of liver regeneration [28]. HCC cell lines like many cancer cell lines display uncontrolled cell proliferation. In order to force HCC cell lines to exit cell cycle by UPR, we treated them with tunicamycin and tested ATAD2 protein levels. As shown in Fig. 3, following 12 h and 24 h treatment with tunicamycin, Hep3B cells displayed early accumulation of CHOP and strong induction of PARP cleavage, as well as downregulation of ATAD2 levels particularly at 24 h. This suggested that tunicamycin treatment caused a cell cycle arrest as well as apoptosis induction. The response of HepG2 cells was milder in terms of PARP cleavage but ATAD2 downregulation was evident at 12 h and strong at 24 h, suggesting minor apoptosis and more pronounced cell cycle exit. In support of our conclusion, we noticed that ATAD2 was one of the significantly downregulated genes in G0 as compared to G1 cells [29]. Taken together our observations supported by other reports are in favor of ATAD2 being a biomarker for a non-resting (non G0) state independent of cell cycle phases.

Next, we examined HCC cell response to *ATAD2* downregulation. Out of five HCC cell lines tested, only two displayed clear and objective survival response (Online Resource 3). Detailed phenotypic analysis of *ATAD2* knock-down effects in four representative cell lines clearly demonstrated that ATAD2 dependency is highly heterogeneous. Although a few HCC cell lines experience decreased survival and cell death, many others do not show any severe survival defect. Our compared global gene expression analysis also indicates extreme heterogeneity in response to ATAD2 deficiency. Cellular response varied between no detectable alterations in gene expression to more than 100 genes affected. Thus, our observations lead us to conclude that ATAD2 expression is not absolutely necessary for survival of HCC cell lines or its effects are dependent on other factors. In other words, the effects of ATAD2 deficiency appear unpredictable in the contexts we analyzed. In accordance with our previous studies we concluded that ATAD2 depletion related survival outcomes do not associate with metastatic (EMT) status of HCC cells, as well as mutations in p53 or Rb pathway. Two out of 4 epithelial cells (Hep3B and HepG2) responded to ATAD2 depletion but the other 2 epithelial lines (PLC/PRF/5 and Huh7) and SNU449, as the only EMT cell line in our panel, did not [30]. Among the responders HepG2 is p53wt, whereas Hep3B is p53 null. Also, all the cell lines used in this study, responders and non-responders, are Rb pathway deficient [31]. Therefore, additional studies are necessary to identify markers of response to ATAD2 depletion.

In support of this conclusion, ATAD2 has been qualified previously as a global “helper” which in growing cells can be compensated for by other factors [2]. When compared to previous reports on the effects of ATAD2 suppression on HCC cell lines, our observations correlate only partially. Indeed, similar

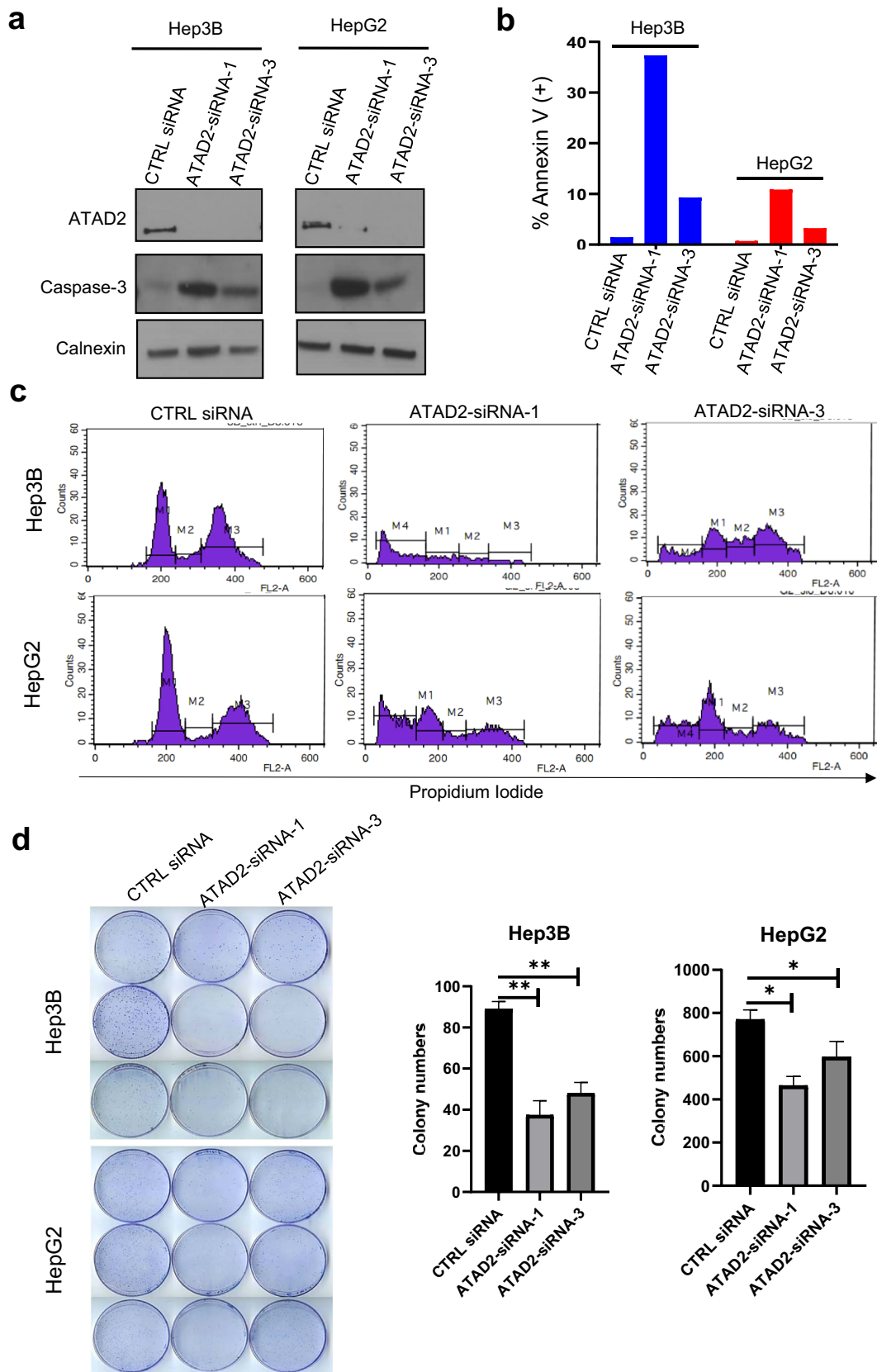


**Fig. 4** Suppression of ATAD2 by siRNAs inhibits cell growth and induces apoptosis. **a** Western blot analysis of ATAD2 protein expression in Hep3B and HepG2 cell lines after transfection of control siRNA, ATAD2 siRNA1 and ATAD2 siRNA3 demonstrates ATAD2 knock-down accompanied by increased expression of active Caspase-3. **b** Annexin V FACS analysis of ATAD2-suppressed Hep3B and HepG2 cells at day 2 shows abundant apoptosis in Hep3B and less but evident apoptosis in HepG2 cells. **c** Cell cycle analysis by flow cytometry at day 3 following siRNA treatment showed strong perturbation of cell cycle phase distribution with increase in SubG1 cells. **d** ATAD2 siRNA-treated cells displayed significant decrease in colony formation ability as shown by Coomassie blue staining (left) and colony number counting (right) or control siRNA transfected Hep3B and HepG2 cell colonies

observations were reported for Hep3B and HepG2 cells [21, 32]. But we could not confirm earlier reports on ATAD2 dependency of Huh7 and PLC/PRF/5 cell lines [21, 32, 33]. The reasons of

this discrepancy are not known. Cell lines used in these studies may have undergone drifts during their long-term maintenance between different laboratories. Alternatively, experimental conditions may have affected the phenotypic outcomes. Nevertheless, it is of interest that ATAD2-independent HCC cell survival has not been noticed in previous reports [21, 32, 33]. Here we show that ATAD2 is not a critical gene for the survival of many different HCC cell lines. These findings strongly suggest that this gene is not a preferable target for development of new targeted therapy approaches for HCC unless its function is further characterized. Indeed, as a gene associated with both normal and malignant cell proliferation, even if successful results can be achieved, such therapies might present undesirable side effects. Altogether, here we show that ATAD2 is an excellent proliferation marker for liver diseases including HCC. However, currently, it is not a preferable therapeutic target.

**Fig. 5** ATAD2 knock-down by doxycycline-induced shRNA expression inhibits Hep3B tumor development in immunodeficient mice. **a** Representative in vivo image of tumors formed by control and ATAD2-deficient Hep3B cells in immunodeficient mice. Hep3B-derived RFP-expressing clones with Doxycycline-induced shATAD2 and shCTRL expression were inoculated into opposite sides of mice ( $n = 3$ ) and tumor formation in doxycycline-fed mice were followed up to 37 days. **b** Western blot analysis of ATAD2 protein levels in shCTRL- and shATAD2-expressing tumors demonstrating efficient inhibition of ATAD2. **c** Tumor growth curves of shCTRL and shATAD2 Hep3B cells based on doxycycline treatment that showed significant inhibition by ATAD2 knock-down ( $p = 0.0064$ )

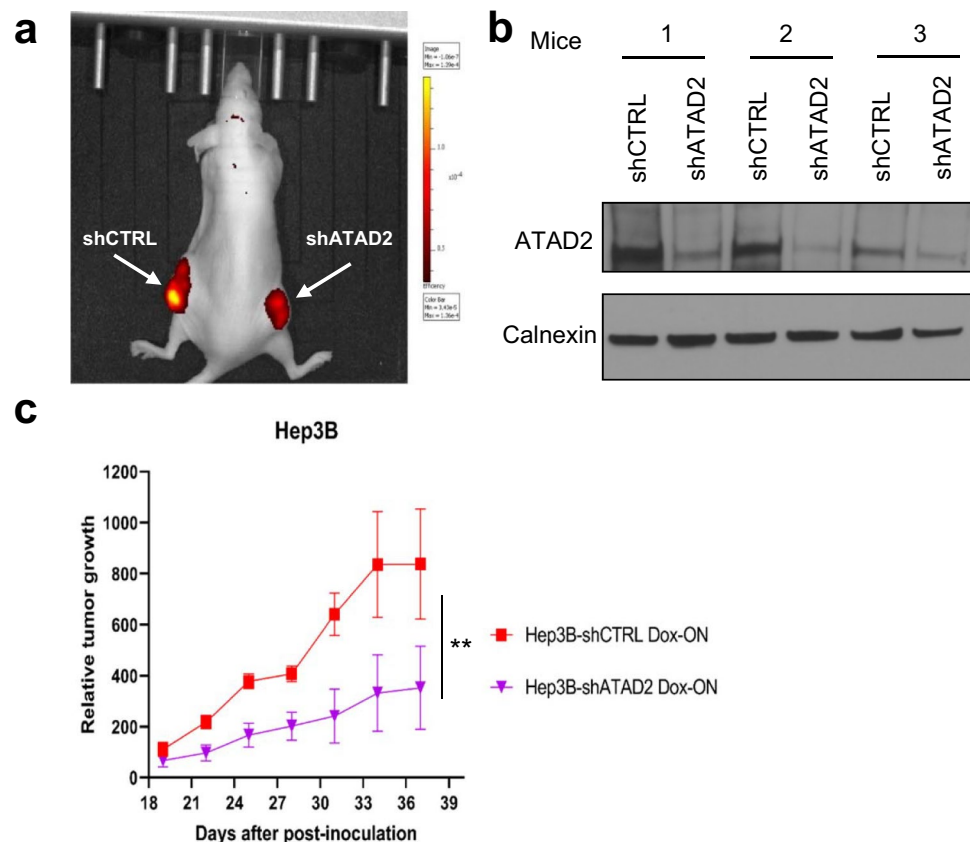


**Fig. 6** Suppression of ATAD2 by siRNAs did not affect cell cycle distribution in Huh7 cell line. **a** Detection of ATAD2 protein expression in Huh7 cell line transfected with control siRNA, ATAD2 siRNA1 or ATAD2 siRNA3 at day 2 by Western blotting. **b** Cell cycle analysis with propidium iodide staining of control siRNA, ATAD2 siRNA1 and ATAD2 siRNA3 transfected Huh7 cell line at day 3. **c** Quantification of cells at different phases of cell cycle showing that there is no consistent change under ATAD2 silencing

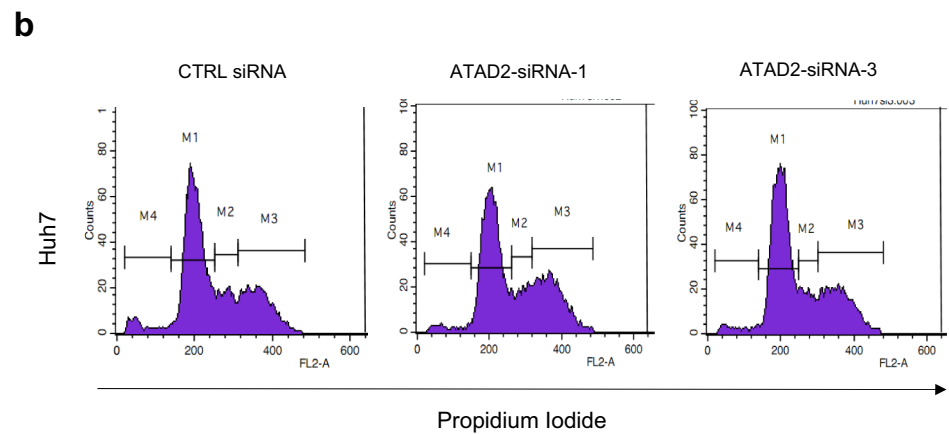
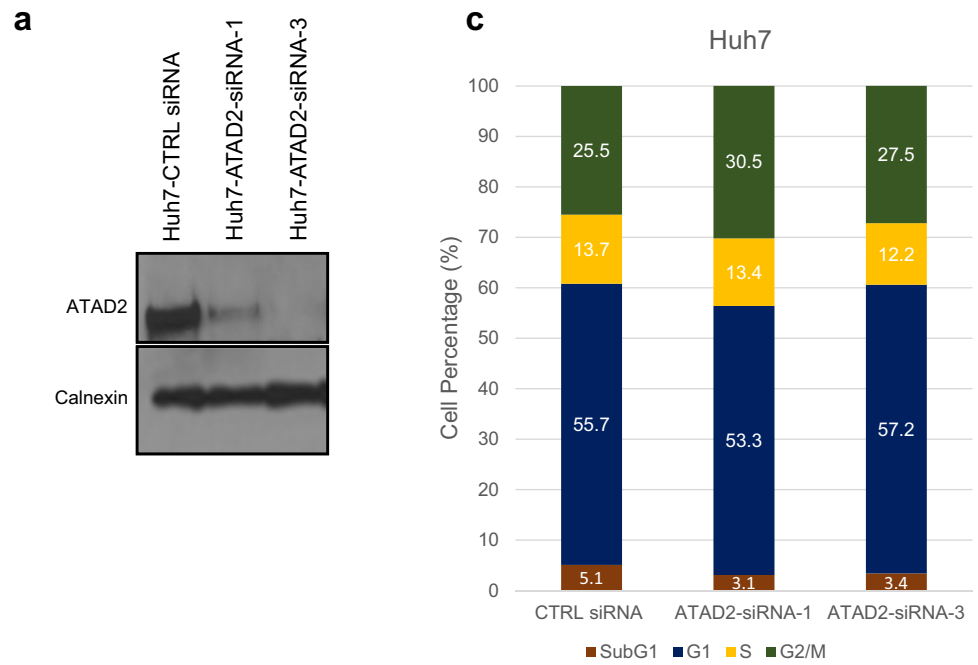


**Table 2** Distribution of genes affected by ATAD2 knockdown in different HCC cell lines

| Cell      | Up | Down | Total |
|-----------|----|------|-------|
| Hep3B     | 54 | 57   | 111   |
| PLC/PRF/5 | 9  | 7    | 16    |
| SNU449    | 0  | 0    | 0     |

**Fig. 7** Demonstration of ATAD2 knock-down by real-time PCR in Hep3B, SNU449, and PLC/PRF/5 prior to transcriptome analysis by microarray



**Table 3** Collapsed gene ontology functions affected by ATAD2 in two HCC cell lines\*

| GO term-based functions                      | GO terms |
|--|----------|
| <b>Hep3B (<i>p</i> Adj. &lt; 0.02)</b>       |          |
| Response to calcium ion                      | 1        |
| Response to metal ion                        | 1        |
| Pos. regulation of protein kinase B sig      | 3        |
| Response to ketone                           | 1        |
| Neg. regulation of blood coagulation         | 11       |
| Response to glucocorticoid                   | 3        |
| Neg. regulation of ion transport             | 1        |
| Response to cAMP                             | 1        |
| Zymogen activation                           | 1        |
| Regulation of apoptotic signaling**          | 1        |
| Regulation of response to wounding           | 1        |
| Organic hydroxy compound transport           | 1        |
| Reg. of heterotypic cell–cell adhesion       | 2        |
| Glomerulus vasculature development           | 1        |
| Kidney vasculature development               | 2        |
| Pos. regulation of hormone secretion         | 1        |
| Response to organophosphorus                 | 1        |
| <b>PLC/PRF/5 (<i>p</i> adj. &lt; 0.05)</b>   |          |
| High-density lipoprotein particle remodeling | 7        |
| Pos. reg. of canonical Wnt signaling pw      | 4        |
| Receptor-mediated endocytosis                | 1        |

\*Full list of related GO terms where presented in Online Resource 4; \*\*Regulation of extrinsic apoptotic signaling pathway via death domain receptors

## Conclusions

In the study, the comparative analysis based on TCGA and immunochemistry strongly indicated that ATAD2 expression increases in HCC tumor samples. The expression of ATAD2 showed a strong correlation with Ki-67 expression in normal liver and HCC. At the cellular level, ATAD2 depletion showed decreased survival in some but not all of HCC cell lines, indicating ATAD2 is not a crucial gene for survival. In addition, comparative gene expression analysis in ATAD2 depleted HCC cell lines showed different types of cellular responses resulted in a cell line dependent manner. The randomness in cellular fate with ATAD2 depletion, and its correlative expression with proliferation markers in regenerating liver, shows ATAD2 needs further explorations as a proliferation biomarker or preferential therapeutic target in clinical use.

**Supplementary Information** The online version contains supplementary material available at <https://doi.org/10.1007/s12029-021-00732-9>.

**Acknowledgements** This work was part of PhD theses of H.Y. (Bilkent University, Ankara, Turkey). We would like to thank Izmir Biomedicine and Genome Center's core facilities especially Optical Imaging and IBG Bioinformatics Platform (IBG-BIP) for their support during data collection and analysis.

**Author Contribution** Study conception and design: MO; experiments: UE, HY, CO, OY, PK, and EB. Bioinformatics and statistical analyses: GK, HU, and UE; evaluation of the data: MO, NA, HA, FY, and PBK; drafting of the manuscript: MO and UE. All authors were involved in finalization of the manuscript and approved the submitted version.

**Funding** This study was supported by the funds from TUBITAK (109S191, 111T558), Turkish Academy of Sciences, Dokuz Eylul University, and Izmir Biomedicine and Genome Center.

**Availability of Data and Material** The contributions for the study are included in the article/Online Resources. Raw microarray data that support the findings of this study and further information are available upon request from corresponding author.

## Declarations

**Ethics Approval** Study with clinical samples was approved by Ege University Ethics Committee. Animal experiments were approved by Bilkent University Animal Ethics Committee. (Decision No: 2006/1; Decision date: 10/5/2006).

**Conflict of Interest** The authors declare no competing interests.

## References

- Cattaneo M, Morozumi Y, Perazza D, Boussouar F, Jamshidikia M, Rousseaux S, Verdel A, Khochbin S. Lessons from yeast on emerging roles of the ATAD2 protein family in gene regulation and genome organization. *Mol Cells*. 2014;37:851–6. <https://doi.org/10.14348/molcells.2014.0258>.
- Morozumi Y, Boussouar F, Tan M, Chaikuad A, Jamshidikia M, Colak G, He H, Nie L, Petosa C, De Dieuleveult M, et al. ATAD2 is a generalist facilitator of chromatin dynamics in embryonic stem cells. *J Mol Cell Biol*. 2016;8:349–62. <https://doi.org/10.1093/jmcb/mjv060>.
- Koo SJ, Fernández-Montalván AE, Badock V, Ott CJ, Holton SJ, von Ahlsen O, Toedling J, Vittori S, Bradner JE, Gorjánác M. ATAD2 is an epigenetic reader of newly synthesized histone marks during DNA replication. *Oncotarget*. 2016;7:70323–35. <https://doi.org/10.18632/oncotarget.11855>.
- Cho C, Jang J, Kang Y, Watanabe H, Uchihashi T, Kim SJ, Kato K, Lee JY, Song JJ. Structural basis of nucleosome assembly by the Abo1 AAA+ ATPase histone chaperone. *Nat Commun*. 2019;10:1–13. <https://doi.org/10.1038/s41467-019-13743-9>.
- Shahnejat-Bushehri S, Ehrenhofer-Murray AE. The ATAD2/ANCCA homolog Yta7 cooperates with Scm3HJURP to deposit Cse4CENP-A at the centromere in yeast. *Proc Natl Acad Sci U S A*. 2020;117:5386–93. <https://doi.org/10.1073/pnas.1917814117>.
- Zou JX, Revenko AS, Li LB, Gemo AT, Chen HW. ANCCA, an estrogen-regulated AAA+ ATPase coactivator for ER $\alpha$ , is required for coregulator occupancy and chromatin modification. *Proc Natl Acad Sci U S A*. 2007;104:18067–72. <https://doi.org/10.1073/pnas.0705814104>.
- Ciró M, Prosperini E, Quarto M, Grazini U, Walfridsson J, McBlane F, Nucifero P, Pacchiana G, Capra M, Christensen J, et al. ATAD2 is a novel cofactor for MYC, overexpressed and amplified in aggressive tumors. *Cancer Res*. 2009;69:8491–8. <https://doi.org/10.1158/0008-5472.CAN-09-2131>.
- Caron C, Lestrat C, Marsal S, Escoffier E, Curtet S, Virolle V, Barbry P, Debernardi A, Brambilla C, Brambilla E, et al.

- Functional characterization of ATAD2 as a new cancer/testis factor and a predictor of poor prognosis in breast and lung cancers. *Oncogene*. 2010;29:5171–81. <https://doi.org/10.1038/onc.2010.259>.
9. Yildiz G, Arslan-Ergul A, Bagislar S, Konu O, Yuzugullu H, Gursoy-Yuzugullu O, Ozturk N, Ozen C, Ozdag H, Erdal E, Karademir S, et al. Genome-wide transcriptional reorganization associated with senescence-to-immortality switch during human hepatocellular carcinogenesis. *PLoS One*. 2013;8. <https://doi.org/10.1371/journal.pone.0064016>.
  10. Hussain M, Zhou Y, Song Y, Hameed HMA, Jiang H, Tu Y, Zhang J. ATAD2 in cancer: a pharmacologically challenging but tractable target. *Expert Opin Ther Targets*. 2018;22:85–96. <https://doi.org/10.1080/14728222.2018.1406921>.
  11. Yuzugullu H, Benhaj K, Ozturk N, Senturk S, Celik E, Toylu A, Tasdemir N, Yilmaz M, Erdal E, Akcali KC, et al. Canonical Wnt signaling is antagonized by noncanonical Wnt5a in hepatocellular carcinoma cells. *Mol Cancer*. 2009;8:90. <https://doi.org/10.1186/1476-4598-8-90>.
  12. Torbenson MS, Ng IOL, Park YN, Roncalli M, Sakamoto M. Hepatocellular carcinoma. In: WHO Classification of Tumors Editorial Board. Digestive system tumours. WHO classification of tumours series. 5th ed. Lyon: Int Agen Res Cancer. 2019:229–39.
  13. Goldman MJ, Craft B, Hastie M, Repčeka K, McDade F, Kamath A, Banerjee A, Luo Y, Rogers D, Brooks AN, et al. Visualizing and interpreting cancer genomics data via the Xena platform. *Nat Biotechnol*. 2020;38:675–8. <https://doi.org/10.1038/s41587-020-0546-8>.
  14. Gautier L, Cope L, Bolstad BM, Irizarry RA. Affy-analysis of Affymetrix GeneChip data at the probe level. *Bioinformatics*. 2004;20:307–15. <https://doi.org/10.1093/bioinformatics/btg405>.
  15. Ritchie ME, Phipson B, Wu D, Hu Y, Law CW, Shi W, Smyth GK. Limma powers differential expression analyses for RNA-seq and microarray studies. *Nucleic Acids Res*. 2015;43:e47. <https://doi.org/10.1093/nar/gkv007>.
  16. Yu G, Wang LG, Han Y, He QY. ClusterProfiler: an R package for comparing biological themes among gene clusters. *Omi A J Integr Biol*. 2012;16:284–7. <https://doi.org/10.1089/omi.2011.0118>.
  17. Edgar R, Domrachev M, Lash AE. Gene Expression Omnibus: NCBI gene expression and hybridization array data repository. *Nucleic Acids Res*. 2002;30:207–10. <https://doi.org/10.1093/nar/30.1.207>.
  18. Brewer JW, Hendershot LM, Sherr CJ, Diehl JA. Mammalian unfolded protein response inhibits cyclin D1 translation and cell-cycle progression. *Proc Natl Acad Sci U S A*. 1999;96:8505–10. <https://doi.org/10.1073/pnas.96.15.8505>.
  19. Banerjee A, Lang JY, Hung MC, Sengupta K, Banerjee SK, Baksi K, Banerjee DK. Unfolded protein response is required in nu/nu mice microvasculature for treating breast tumor with tunicamycin. *J Biol Chem*. 2011;286:29127–38. <https://doi.org/10.1074/jbc.M110.169771>.
  20. Yang J, Huang J, Luo L, Chen Z, Guo Y, Guo L. Significance of PRO2000/ANCCA expression, a novel proliferation-associated protein in hepatocellular carcinoma. *Cancer Cell Int*. 2014;14:1–7. <https://doi.org/10.1186/1475-2867-14-33>.
  21. Huang J, Yang J, Lei Y, Gao H, Wei T, Luo L, Zhang F, Chen H, Zeng Q, Guo L. An ANCCA/PRO2000-miR-520a-E2F2 regulatory loop as a driving force for the development of hepatocellular carcinoma. *Oncogenesis*. 2016;5:e229. <https://doi.org/10.1038/oncsis.2016.22>.
  22. Hwang HW, Ha SY, Bang H, Park CK. ATAD2 as a poor prognostic marker for hepatocellular carcinoma after curative resection. *Cancer Res Treat*. 2015;47:853–61. <https://doi.org/10.4143/crt.2014.177>.
  23. Kaita KDE, Pettigrew N, Minuk GY. Hepatic regeneration in humans with various liver disease as assessed by Ki-67 staining of formalin-fixed paraffin-embedded liver tissue. *Liver*. 1997;17:13–6. <https://doi.org/10.1111/j.1600-0676.1997.tb00772.x>.
  24. Gerlach C, Sakkab DY, Scholzen T, Daßler R, Alison MR, Gerdes J. Ki-67 expression during rat liver regeneration after partial hepatectomy. *Hepatology*. 1997;26:573–8. <https://doi.org/10.1053/jhep.1997.v26.pm0009303485>.
  25. Gerdes J, Schwab U, Lemke H, Stein H. Production of a mouse monoclonal antibody reactive with a human nuclear antigen associated with cell proliferation. *Int J Cancer*. 1983;31:13–20. <https://doi.org/10.1002/ijc.2910310104>.
  26. Cuylen S, Blaukopf C, Politi AZ, Muller-Reichert T, Neumann B, Poser I, Ellenberg J, Hyman AA, Gerlich DW. Ki-67 acts as a biological surfactant to disperse mitotic chromosomes. *Nature*. 2016;535:308–12. <https://doi.org/10.1038/nature18610>.
  27. Bassik MC, Kampmann M. Knocking out the door to tunicamycin entry. *Proc Natl Acad Sci U S A*. 2011;108:11731–2. <https://doi.org/10.1073/pnas.1109035108>.
  28. Lai S-S, Zhao D-D, Cao P, Lu K, Luo O-Y, Chen W-B, Liu J, Jiang E-Z, Yu Z-H, Lee G, et al. PP2A $\alpha$  positively regulates the termination of liver regeneration in mice through the AKT/GSK3 $\beta$ /Cyclin D1 pathway. *J Hepatol*. 2016;64:352–60. <https://doi.org/10.1016/j.jhep.2015.09.025>.
  29. Oki T, Nishimura K, Kitaura J, Togami K, Maehara A, Izawa K, Sakae-Sawano A, Niida A, Miyano S, Aburatani H, Kiyonari H, et al. A novel cell-cycle-indicator, mVenus-p27K<sup>-</sup>, identifies quiescent cells and visualizes G0-G1 transition. *Sci Rep*. 2014;4. <https://doi.org/10.1038/srep04012>.
  30. Sreekumar R, Emaduddin M, Al-Saihati H, Moutasim K, Chan J, Spampinato M, Bhome R, Yuen HM, Mescoli C, Vitale A, Cillo U, et al. Protein kinase C inhibitors override ZEB1-induced chemoresistance in HCC. *Cell Death Dis*. 2019;10. <https://doi.org/10.1038/s41419-019-1885-6>.
  31. Sayan AE, Sayan BS, Findikli N, Ozturk M. Acquired expression of transcriptionally active p73 in hepatocellular carcinoma cells. *Oncogene*. 2001;20:5111–7. <https://doi.org/10.1038/sj.onc.1204669>.
  32. Lu WJ, Chua MS, So SK. Suppression of ATAD2 inhibits hepatocellular carcinoma progression through activation of p53- and p38-mediated apoptotic signaling. *Oncotarget*. 2015;6:41722–35. <https://doi.org/10.18632/oncotarget.6152>.
  33. Wu G, Liu H, He H, Wang Y, Lu X, Yu Y, Xia S, Meng X, Liu Y. MiR-372 down-regulates the oncogene ATAD2 to influence hepatocellular carcinoma proliferation and metastasis. *BMC Cancer*. 2014;14:1–11. <https://doi.org/10.1186/1471-2407-14-107>.